Malaysian Journal of Chemistry, 2025, Vol. 27(3), 340-352
(Special Issue: *International Conference on Sustainable Materials and Technologies, ICSMT 2025*)

Glucose-Mediated Synthesis of Copper Nanowires for the Selective and Sensitive Electrochemical Determination of Paracetamol

M. Gokula Krishnan[1], A. Sethumadavan[1], K. Ganesan[2], P. Muthukumar[3], A. John Jeevagan[1], T. Adinaveen[4] and M. Amalraj[1]*

[1]Department of Chemistry, Arul Anandar College (Autonomous), Karumathur, Madurai, Tamil Nadu, India.
[2]Department of Chemistry, Thiagarajar College, Madurai, Tamil Nadu, India
[3]Department of Chemistry, Bannari Amman Institute of Technology, Erode, Tamil Nadu, India-638401
[4]Department of Chemistry, Loyola College, Nungambakkam. Chennai, Tamil Nadu, India
*Corresponding author (e-mail: amalraj@aactni.edu.in)

The exceptional properties of copper nanowires (CuNWs) including high electrical conductivity, strong optoelectronic performance, and excellent mechanical strength make them highly valuable for diverse applications across various fields. Herein we report the synthesis of CuNWs using surfactant assisted glucose reduction method. The concentration of surfactant hexadecylamine (HDA) and glucose concentrations were optimized to obtain nanowire morphology. The as prepared CuNWs were characterized using UV-visible spectroscopy (UV-vis) and FT-IR spectroscopy and scanning electron microscopy (SEM). UV-vis and SEM studies confirmed the variation of aspect ratio of the CuNWs with respect to the concentration of HDA. Further, copper nanowires (CuNWs) were deposited onto a glassy carbon electrode (GCE) using the drop-casting technique to investigate their electrocatalytic activity. The modified electrode was characterized through cyclic voltammetry. The active electrochemical surface area of the CuNWs-modified electrode was determined using the Anson equation and was calculated to be 0.031 cm^2. Furthermore, the electrochemical oxidation of paracetamol (PA) was investigated using both bare and CuNWs-modified glassy carbon electrodes (GCE) at pH 7.2. The CuNWs-modified GCE exhibited a fourfold enhancement in the oxidation current of PA compared to the bare GCE, indicating significantly improved electrocatalytic activity. Selective detection of PA was successfully achieved even in the presence of a 100-fold excess concentration of ascorbic acid (AA), demonstrating excellent selectivity. Additionally, the sensitivity and limit of detection (LOD) for PA at the CuNWs-modified GCE were assessed using amperometric measurements. The modified electrode was capable of detecting PA concentrations as low as 30 nM at pH 7.2.

Keywords: Copper nanowires; glucose reduction; drop casting; Chronocoulometry; electrochemical sensor

Received: February 2025; Accepted: April 2025

In recent years, the applications of nanostructured materials based on metals, metal oxides, semiconductors, carbon-based materials, and polymeric nanocomposites have been extensively explored. [1, 2]. In consequence of their properties and wide range of application, one dimensional nanostructured materials (1D) including nanofibers, nanowires and nanotubes have received more attention among the researchers [3-6]. The unique attributes of one-dimensional (1D) nanostructured materials such as their exceptional surface-to-volume ratio, tunable thermal and transport properties, and inherently high surface area have positioned them as vital components across a broad spectrum of applications, including electronics, optoelectronics, photonics, magnetism, catalysis, energy conversion, and chemical sensing. [7-11]. Because of its extraordinary electrical conductivity and thermal conductivity, copper is known as one the most promising industrial metal and it has been widely used in various fields including automobile, electronics, machinery and aerospace [12,13]. Though silver has superior conductivity, the insufficient resource and high cost, the usage of silver-based materials are limited [14, 15].

Like gold and silver, copper nanomaterials also exhibit unique optical, mechanical, electrical, and catalytic properties compared to their bulk counterparts [16, 17]. Since copper nanomaterials are low cost and highly conductive, they have been proposed as promising candidate for many future applications, which is impossible by gold and silver. Different shaped copper nanomaterials including nanoparticles, nanorings, nanorods, nanocubes, nanoplates and nanowires (NWs) have been successfully synthesized by many researchers [18-22]. Among the various copper nanomaterials, on account of their exclusive properties such as high

†Paper presented at the International Conference on Sustainable Materials and Technologies (ICSMT 2025)

aspect ratio, highly efficient electron transfer and low annealing temperature, copper nanowires (CuNWs) have been extensively studied by various researchers [23-26]. In recent years, CuNWs have been used for various electronic applications including flexible transparent conductive electrode, photodetectors, field emission devices, photodetectors, electrical interconnects, gas sensors, field emission devices, microheaters, lithium-ion battery and stretchable electrode [27-30].

Several approaches, including template-assisted electrochemical methods, electrospinning, chemical vapor deposition, chemical-solution methods (CSMs), vacuum thermal decomposition, hydrothermal synthesis, precursor solution reduction, and catalytic synthesis, are commonly used as mainstream routes for the synthesis of nanowires (NWs) [31-37]. Among the various methods, because of their less complicated processing, energy efficiency, low cost and no need of toxic chemicals and valuable catalyst, soft hydrothermal synthetic method are widely used for scalable and controllable preparation of CuNWs [38, 39]. To date, extensive efforts have been devoted to the synthesis of copper nanowires (CuNWs) via the hydrothermal method. Notably, Wang et al. achieved the fabrication of highly uniform CuNWs with an average diameter of 35 nm and a length of approximately 100 μm by employing octyldiamine (ODA) as a capping agent and ascorbic acid as a mild reducing agent. This approach highlights the effectiveness of controlled chemical environments in tailoring nanowire morphology and dimensions. [40]. Hwang et al. reported the synthesis of ultra-long copper nanowires (CuNWs) exhibiting an average length of 92.5 μm and a diameter of approximately 47 nm, achieved through a finely tuned hydrothermal process conducted in a water–alcohol mixed solvent system. In this approach, L-ascorbic acid functioned as a effective reducing agent, while oleylamine acted as a surface-coordinating ligand, promoting anisotropic growth and enabling precise control over the nanowire morphology and aspect ratio [41]. Mayousse et al established the simple hydrothermal protocol for the synthesis of CuNWs using octadecayl amine [42]. Zheng et al prepared the long CuNWs with high aspect ratio using oleylamine-mediated hydrothermal synthesis with average diameter of 80nm [43]. Aziz et al synthesized the CuNWs by simple hydrothermal method using hexadecaylamine (HAD) and potassium bromide as capping agent [44]. Though several attempts have made by researchers, the synthesis of pure and high yield CuNWs through wet-chemical methods is still challenging. Hence, it is attempted to optimize and control the growth of CuNWs using the soft template hexadecyl amine (HDA) which also acts as stabilizing agent and glucose as the reducing agent in high yield and to utilize them as an electrode material.

Due to its analgesic and antipyretic properties, paracetamol (PA) is widely used as an effective medication for reducing fever and relieving pain associated with conditions such as backache, headache, postoperative discomfort, and arthritis [45]. Furthermore, owing to its lack of anti-inflammatory effects, paracetamol (PA) has been widely recognized as a household medication for over three decades. At standard therapeutic doses, PA undergoes rapid and complete metabolism primarily through glucuronidation and sulfation pathways, with the resulting inactive metabolites excreted via the urine [46]. While paracetamol (PA) is typically metabolized efficiently at therapeutic doses, an overdose can lead to the accumulation of harmful metabolites in the body. This build-up can cause severe damage to the liver (hepatotoxicity) and kidneys (nephrotoxicity), posing significant health risks [47]. Consequently, the determination of paracetamol (PA) in biological fluids has gained increasing significance.

Herein we report the hydrothermal method for the preparation of well dispersed and ultra-long CuNWs with uniform diameters in the range of 60–160 nm. In this study, we used hexadecylamine (HDA) as both a capping and shape-directing agent, with glucose serving as the reducing agent. The synthesized copper nanowires (CuNWs) were thoroughly characterized using UV-visible and infrared (IR) spectroscopy. The morphology of the CuNWs was meticulously examined using scanning electron microscopy (SEM). Subsequently, the CuNWs were immobilized onto the surface of a glassy carbon electrode (GCE), and the electrochemical behavior of the modified electrode was investigated using cyclic voltammetry. The active electrochemical surface area covered by CuNWs was calculated using chronocoloumetry. Furthermore, the electrocatalytic behavior of the CuNWs-modified GCE was investigated through the oxidation of paracetamol (PA). The CuNWs-modified GCE demonstrated significantly enhanced electrocatalytic activity and superior stability compared to the bare GCE in the oxidation of PA. The selective determination of PA was evaluated in the presence of a 100-fold excess concentration of ascorbic acid (AA). To assess the sensitivity of the electrode toward PA, amperometric analysis was performed. The modified electrode exhibited both high sensitivity and selectivity for PA detection across a wide concentration range, attributed to the increased surface area and active electrochemical surface area of the CuNWs.

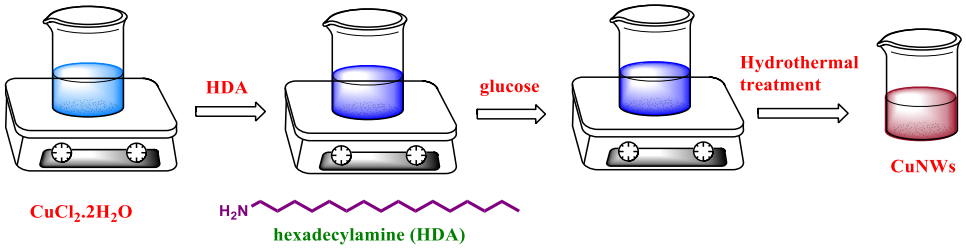

Figure 1. Schematic representation of the preparation process for CuNWs.

MATERIALS AND METHODOLOGY

Chemicals and Materials

Analytical grade chemicals were purchased and used without further purification. $CuCl_2.2H_2O$ (Fisher scientific, Qualigens fine chemicals), 1-Hexadecylammine (HDA, Sigma-Aldrich), β-D-glucose (Merck), ethanol (Merck), acetone (Merck), sodium hydrogen phosphate ($NaHPO_4$) (Merck), sodium dihydrogen phosphate (NaH_2PO_4) (Merck) and sodium hydroxide (Merck) were used as received. 0.2 M phosphate buffer solution (PBS) was prepared using $NaHPO_4$ and NaH_2PO_4. All stock solutions were prepared using ultrapure double-distilled water. All other reagents employed in this study were of analytical grade and were used directly, without any further purification.

Instrumentation

Electrochemical measurements were performed using a conventional three-electrode system. In this setup, a glassy carbon electrode (GCE) served as the working electrode, a platinum wire was employed as the counter electrode, and a KCl-saturated Ag/AgCl electrode functioned as the reference electrode. These electrochemical experiments were conducted using a CHI600E electrochemical analyzer (Austin, TX, USA), which facilitated precise measurements of the electrochemical behavior. Additionally, UV–visible absorption spectra were acquired using a JASCO V630 UV–visible Spectrophotometer to analyze the optical properties of the samples. FT-IR spectra were obtained using a JASCO FT-IR spectrometer, with potassium bromide (KBr) serving as the reference material. These spectra provided valuable information on the functional groups and chemical bonding within the samples. In addition, scanning electron microscopy (SEM) measurements were carried out using a VEGA3 TESCAN SEM (USA), which allowed for high-resolution imaging of the sample morphology and surface structure. For differential pulse voltammetry (DPV) measurements, the following parameters were used. Amplitude - 0.05 V, pulse width - 0.06 s, sample width - 0.02 s and pulse period of 0.2 s.

Synthesis of CuNWs

CuNWs was synthesized using the surfactant assisted synthesis using glucose as a reducing agent [48,49]. In brief, 105 mg of $CuCl_2 \cdot 2H_2O$, 250 mg of glucose, and 900 mg of HDA were dissolved in 50 mL of deionized water and magnetically stirred at room temperature overnight. The resulting solution was then transferred to an autoclave and heated in an oven at 100 °C for 6 hours. After this, the autoclave was allowed to cool. Then, the resulting red colored colloidal solution was filtered and washed with ethanol and water. The resulting sample was dried in an air oven and used for further characterization. Figure 1 illustrates the synthesis of CuNWs by surfactant assisted glucose reduction method.

Preparation of CuNWs Modified GCE

Before modification, the GCE with a diameter of 0.3 mm, was carefully polished using a 0.5 µm alumina slurry to achieve a smooth and uniform surface. After polishing, the electrode was thoroughly rinsed with distilled water to remove any residual particles. The cleanliness of the polished GCE was then evaluated by conducting an electrochemical test using a 1 mM solution of potassium ferricyanide ($K_3[Fe(CN)_6]$) in the presence of 0.1 M KCl, ensuring the electrode's surface was free from contaminants that could affect the subsequent measurements. The polished electrode surface was allowed to dry at room temperature. The as-synthesized copper nanowires (CuNWs) were carefully re-dispersed in distilled water to ensure a uniform suspension. A measured volume of this dispersion was then drop-cast onto the pre-cleaned surface of the glassy carbon electrode (GCE). The electrode was subsequently left undisturbed at room temperature to allow the solvent to evaporate naturally. This process resulted in the formation of a uniform CuNWs-modified glassy carbon electrode (GCE/CuNWs), ready for electrochemical analysis.

Calculation of Electroactive Surface Area

The electroactive surface area of the CuNWs-modified electrode was quantitatively determined using a standard electrochemical method, employing the following equation to calculate the surface area from the obtained experimental data [50].

$$A = \frac{a}{2nFCD^{1/2}\pi^{1/2}} \qquad (i)$$

Where, 'a' is the slope obtained from the linear portion of the Anson plot (Q vs $t^{1/2}$), 'F' denotes Faraday's constant, 'n' represents the number of electrons involved in the redox process, while 'C' and 'D' correspond to the bulk concentration of the redox couple (1 mM) and its diffusion coefficient (8.4×10^{-6} cm^2 s^{-1}), respectively [51].

RESULTS AND DISCUSSION

Growth of Copper Nanowires

CuNWs were synthesized using HDA at two different concentrations, with glucose as a reducing agent, under hydrothermal conditions. To facilitate the rapid synthesis of CuNWs at a lower temperature than that used in earlier methods employing octadecylamine (ODA) and oleylamine (OLA), glucose was utilized as an external reducing agent. [52,53]. Based on earlier reports, the concentrations of the copper precursor and glucose were kept constant, and the role of HDA in the growth of CuNWs was initially examined in the present investigation. Initially, it was attempted to synthesize copper nanostructures from $CuCl_2$. $2H_2O$ in the absence of either HDA or glucose. It is observed that when either HDA or glucose was absent, the solution persisted blue and no metallic Cu precipitates (Cu^0) were formed. The formation of copper nanostructures (change of colour from blue to reddish brown) was only formed when both HDA and glucose were added in sufficient amounts [54]. Though it is known that glucose itself is able to reduce Cu^{2+} ions to Cu^+ in Benedict's and Fehling's tests, it does not able to reduce Cu^{2+} to Cu^0. It was initially suggested that glucose alone did not act as the reducing agent. In contrast, previous studies reported that the formation of Cu^0 with HDA occurred only at significantly higher temperatures (above 180 °C). [55]. To decrease the operating temperature, it is attempted to use both glucose and HDA for the synthesis of CuNWs. The surfactant hexadecylamine (HDA) plays a crucial role in directing the growth of anisotropic copper nanostructures. In this study, the concentrations of $CuCl_2 \cdot 2H_2O$ and glucose were maintained at 37 mM and 6 mM, respectively. The concentration of HDA was fixed as 90 mM and 180 mM. Initially, Cu^{2+} ions, glucose and HDA were mixed together, stirred overnight and transferred to autoclave. The autoclaves were maintained at 102 °C for 6 hours. A color change from blue to reddish brown signified the formation of copper nanostructures. Hence, the concentrations of both surfactants (HDA) and the reducing agent glucose were optimized to prepare CuNWs with two different aspect ratios [56-58]. The copper nanostructures synthesized using 90 mM HDA and 180 mM HDA were termed as CuNPs-1 and CuNPs-2.

Characterization by UV-visible Spectroscopy

The as-synthesized copper nanowires (CuNWs) were characterized using UV–visible spectroscopy, as illustrated in Figure 2. Metal nanostructures, such as CuNWs, typically exhibit distinct absorption bands in the UV–visible region, which can be attributed to the excitation of surface plasmon resonance (SPR) or interband electronic transitions. These spectral features provide valuable insights into the optical properties, size, and structural uniformity of the synthesized nanomaterials. SPR is a characteristic feature indicative of the metallic nature of the particles. The broad SPR band was observed at 448 nm for CuNPs-1 (curve a) indicating the anisotropic growth of copper nanostructures rather than copper nanospheres. On the other hand, CuNPs-2 shows a shoulder peak at 552 nm and a sharp SPR band at 635 nm (curve b) which may be due to the transverse and longitudinal bands of CuNWs [42]. The differences in position of the SPR band of the CuNPs are mainly due to the effect of shape and size [35]. It can also be noted that there is red-shift of the SPR band in the case of the CuNPs-2. Hence, it is concluded that HDA concentration of 180 mM is essential for the growth of CuNWs.

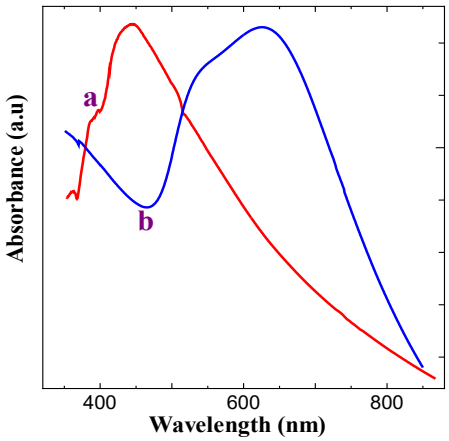

Figure 2. UV-visible spectra obtained for CuNPs prepared using (a) 90 mM and (b) 180 mM HDA.

Characterization by FT-IR Spectroscopy

The HDA assisted copper nanostructures were further characterized using FT-IR spectroscopy. Figure 3 shows the FT-IR spectrum of CuNWs prepared using 180 mM HDA. The appearance of doublet at 2922 and 2851 cm^{-1} indicates the asymmetric and symmetric stretching of C-H bonds of HDA (-CH_2 or -CH_3 group), respectively. The FT-IR spectrum exhibited a characteristic doublet at 3175 and 3250 cm^{-1}, which corresponds to the symmetric and asymmetric stretching vibrations of the primary amine group present in hexadecylamine (HDA). A broad absorption band observed around 3429 cm^{-1} is attributed to the –OH stretching vibrations, indicating the presence of hydroxyl functionalities from β-D-glucose. Additionally, a distinct peak at 1613 cm^{-1} is associated with N–H bending vibrations, further confirming the presence of amine groups. The absorption bands at 1460 and 1377 cm^{-1} are assigned to the bending vibrations of C–H bonds in –CH_2 and –CH_3 groups of HDA, respectively, supporting the successful incorporation of the surfactant into the synthesized nanostructures. The assignments of CuNWs were summarized in table 1.

Morphological characterization by SEM

The morphology of the as-synthesized copper nanostructures (CuNPs) was examined using scanning electron microscopy (SEM). Figures 4 and 5 show the SEM images of CuNWs synthesized using hexadecylamine (HDA) at two different concentrations 90 mM and 180 mM, respectively. Figure 4 illustrates the SEM results for the sample synthesized with 90 mM HDA. From these images, it is evident that the formation and elongation of copper nanowires (CuNWs) are minimal at this concentration. The limited nanowire development suggests that 90 mM of HDA is insufficient to direct or sustain the anisotropic growth necessary for well-defined CuNW formation, indicating the need for a higher surfactant concentration to achieve complete nanowire synthesis. Figure 5A and 5B shows the SEM images obtained for CuNPs prepared using 180 mM HDA with low and high magnification. The SEM images revealed that the final product consists of a large number of copper nanowires with uniform diameters. From the UV-vis spectroscopy and SEM studies, it is concluded that HDA concentration of 180 mM is the optimum concentration for the growth of CuNWs in high yield.

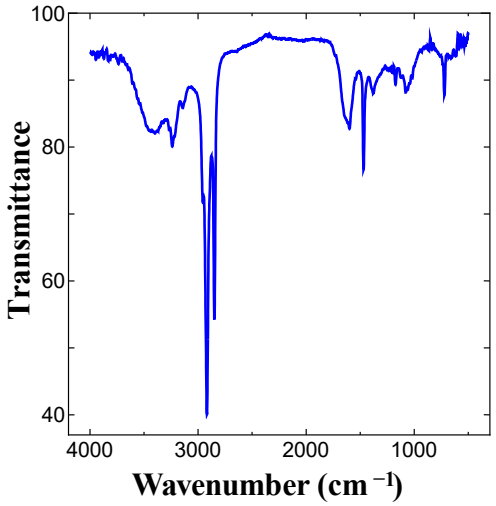

Figure 3. FT-IR spectrum obtained for CuNWs.

Table 1. FT–IR spectral data.

Band position (cm^{-1})	Assignments [59]
2851	ν (C–H) Symmetric (HDA)
2922	ν (C–H) Asymmetric (HDA)
3175	ν (N–H) Symmetric (HDA)
3250	ν (N–H) Asymmetric (HDA)
1613	ν (N–H) Bending (HDA)
1460	ν (C–H) Bending of CH_2 (HDA)
1377	ν (C–H) Bending of CH_3 (HDA)

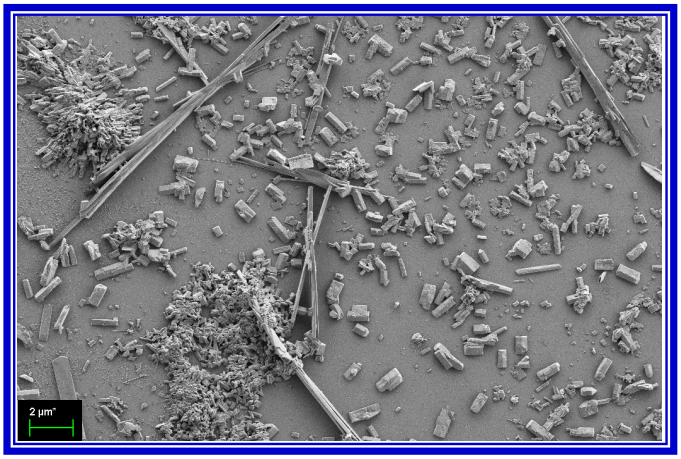

Figure 4. SEM image obtained for CuNPs prepared using 90 mM HDA.

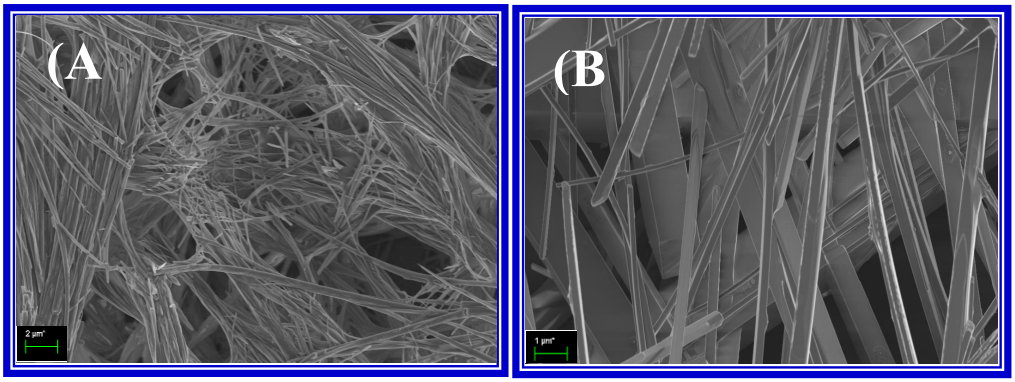

Figure 5. SEM images obtained for CuNWs prepared using 180 mM HDA (A) low magnification, (B) high magnification.

Characterization of GCE/CuNWs by Cyclic Voltammetry

The CuNWs were dispersed in water and then drop casted in a well-cleaned GCE. The dispersion was left to dry at room temperature and subsequently characterized using cyclic voltammetry (CV). Figure 6 presents the cyclic voltammograms (CVs) recorded for both the bare GCE and the CuNWs-modified GCE (GCE/CuNWs) in 0.1 M NaOH solution at a scan rate of 50 mV s^{-1}. As shown in curve (a), the bare GCE does not exhibit any noticeable redox peaks within the investigated potential window, indicating its limited electrochemical activity under these conditions. In contrast, curve (b) corresponding to the GCE/CuNWs reveals a well-defined anodic peak at 0.285 V and a cathodic peak at 0.172 V, resulting in a peak-to-peak separation of 113 mV. This pronounced redox behavior confirms the enhanced electrochemical activity of the CuNWs-modified electrode, attributed to the high conductivity and increased surface area provided by the nanowire structure. The anodic peak is owing to the formation of CuO(OH) from CuNWs and cathodic peak is due to the formation of CuO from CuO(OH). During the anodic scan, the CuO(OH) is formed from CuNWs which will be reduced to CuO rather than Cu^0 in the cathodic scan. Since CuO is more stable, the reduction of CuO(OH) to Cu^0 is not feasible in the potential range [60,61]. The possible reaction mechanism for the redox process during conversion of copper to copper hydroxide is as follows.

$$2Cu + 2OH^- \rightarrow Cu_2O + H_2O + 2e^- \quad [ii]$$

$$Cu_2O + 2OH^- \rightarrow 2CuO + OH^- + 2e^- \quad [iii]$$

$$CuO + OH^- \rightarrow CuOOH + e^- \quad [iv]$$

The formation of CuO from CuOOH follows the following reaction

$$CuOOH + e^- \rightarrow CuO + OH^- \quad [v]$$

Calculation of Active Electrochemical Surface Area

Further, the electrochemically active surface area of GCE/CuNWs was determined using the Anson equation (i). The slope value is obtained from Anson plot (plotted using chronocoulometry: plot of $t^{1/2}$ vs. Q; Slope is calculated from the linear portion of the plot) (Figure 7). The electrochemically active surface area was determined to be 0.031 cm^2.

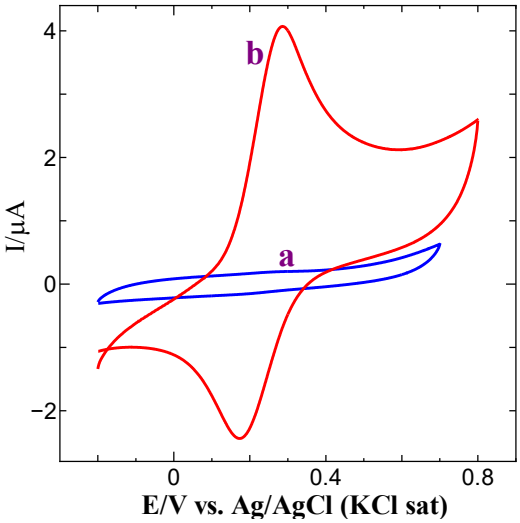

Figure 6. CVs recorded for (a) bare GCE and (b) GCE/CuNWs in 0.1 M NaOH solution at a scan rate of 50 mVs^{-1}.

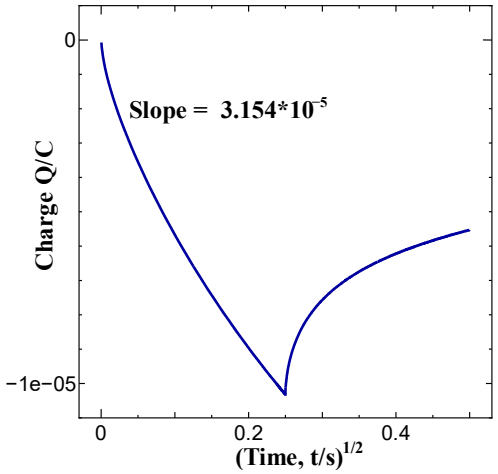

Figure 7. Chronocoulumetry obtained for GCE/CuNWs in 1 mM $K_4[Fe(CN)_6]$ in 0.1 M KCl solution. Pulse Width = 0.25 s.

Electrochemical Oxidation of PA at GCE/CuNWs

The electrocatalytic performance of the CuNWs-modified glassy carbon electrode (GCE/CuNWs) was evaluated using paracetamol (PA) as an electrochemical probe. Figure 8 illustrates the cyclic voltammograms (CVs) recorded for 0.5 mM PA at both the bare GCE and the GCE/CuNWs in 0.2 M phosphate-buffered saline (PBS) with a pH of 7.2. As depicted in curve (a: solid line), the bare GCE exhibits an oxidation peak for PA at approximately 0.57 V. However, during the subsequent potential cycle, this oxidation peak shifts to a more positive potential and the corresponding peak current significantly decreases (curve a: dotted line). This behavior indicates sluggish electron transfer kinetics and reduced electrochemical stability at the unmodified electrode surface. This behavior is attributed to the adsorption of the oxidized product of PA on the GCE surface, leading to surface fouling. In contrast, for the GCE/CuNWs, PA oxidation occurs at 0.56 V, showing a significantly enhanced oxidation peak current (~5-fold) compared to the bare GCE electrode (curve b: solid line). The oxidation potential and oxidation peak current remains unaffected even after several potential cycles (curve b: dotted line). The observed 5-fold increase of PA oxidation current might be because of the high surface area of CuNWs, that catalysis the oxidation of PA. This indicates that GCE/CuNWs acts as an electrocatalyst towards the oxidation of PA and decreases the surface fouling effect caused by the oxidation products of PA. Curve c shows the CV of GCE/CuNWs in 0.2 M PBS in the absence of PA. The high increase in the PA oxidation current might be due to the high electrocatalytic surface area provided by CuNWs compared to the bare GCE.

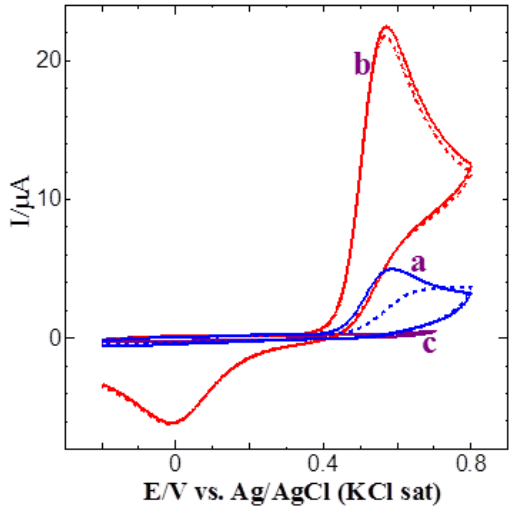

Figure 8. CVs obtained for 0.5 mM PA at (a) bare GCE and (b) GCE/CuNWs in 0.2 M PBS solution (pH 7.2) at a scan rate of 50 mV s^{-1}. Solid line: 1st cycle; Dotted line: 6th cycle. (c) CVs obtained for GCE/CuNWs in 0.2 M PBS (pH 7) in the absence of PA at a scan rate of 50 mV s^{-1}.

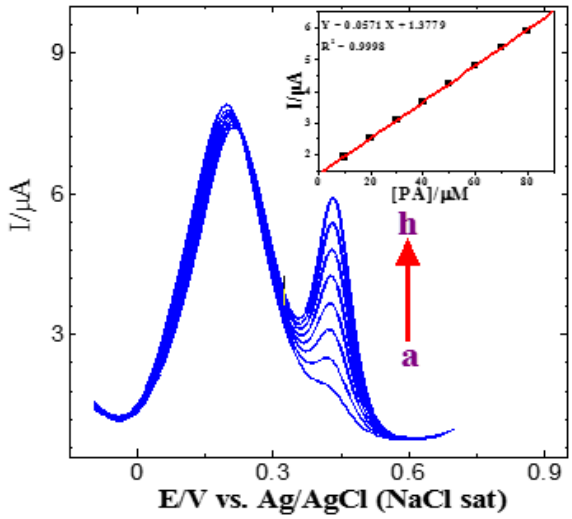

Figure 9. DPVs obtained for each increment of 10 μM PA in the presence of 1 mM AA at CuNWs/GCE in 0.2 M PB solution (pH 7.2). Inset: Plot of concentration Vs. oxidation peak current of PA.

Selective Determination of PA

The electrochemical determination of PA in real sample analysis is mainly hindered by the high concentrations of AA and hence the selective determination of PA in the presence of high concentration of AA is significant. Figure 9 displays the differential pulse voltammograms (DPVs) recorded for the selective detection of 10 μM paracetamol (PA) in the presence of a significantly higher concentration (1 mM) of ascorbic acid (AA). Despite the presence of this 100-fold excess of AA, the sensor demonstrates excellent selectivity, as evidenced by a consistent increase in the oxidation peak current corresponding to PA with each successive addition of 10 μM PA. Notably, the oxidation potential of PA remains unchanged, indicating minimal interference from AA and confirming the high specificity of the modified electrode. The inset of Figure 9 shows a calibration plot of PA concentration versus its oxidation peak current, which reveals a strong linear relationship with a correlation coefficient (R^2) of 0.9998, highlighting the sensor's remarkable sensitivity and linear response over the tested concentration range. On the other hand, the oxidation potential of AA shows only a slight shift, along with a small decrease in the oxidation current with each addition of PA. This suggests that the CuNWs modified electrode exhibits strong selectivity for the determination of PA, even in the presence of 100-fold higher concentrations of AA. Therefore, this electrode can be used for the selective determination of PA in the presence of AA in real sample analysis at physiological pH.

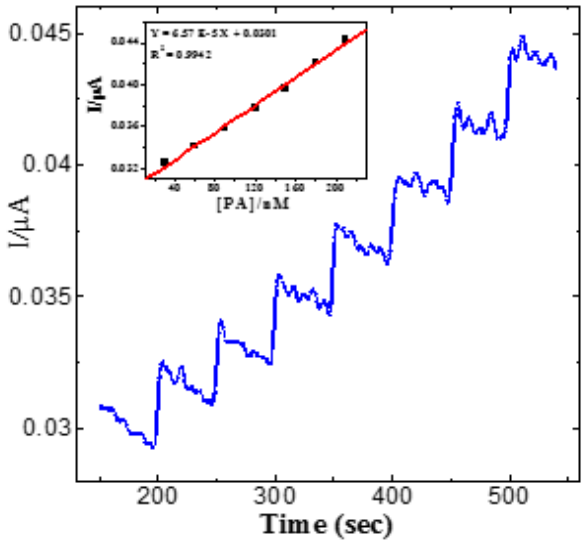

Figure 10. Amperometric i-t curve obtained for 30 nM addition of PA in a regular time interval of 50 s at a constant potential 0.55 V in 0.2 M PB solution. Inset: Plot of concentration versus the oxidation peak current of PA.

Amperometric Determination of PA at CuNWs Modified GCE

Further, the sensitivity of the CuNWs modified GCE towards the electrochemical determination of PA was evaluated using amperometric analysis. Figure 10 illustrates the amperometric i-t response recorded for the successive additions of 30 nM paracetamol (PA) at fixed time intervals of 50 seconds, while maintaining a constant applied potential of 0.55 V. With each incremental addition of 30 nM PA, a corresponding rise in the current response is observed, which rapidly stabilizes within approximately 3 seconds, indicating the rapid and efficient electrocatalytic activity of the modified electrode. The inset of Figure 10 presents the calibration plot of PA concentration versus the steady-state oxidation current, showing a well-defined linear relationship with a correlation coefficient (R^2) of 0.9942. This excellent linearity confirms the high sensitivity and reliability of the CuNWs-modified glassy carbon electrode (GCE) for the accurate detection of ultra-low concentrations of PA.

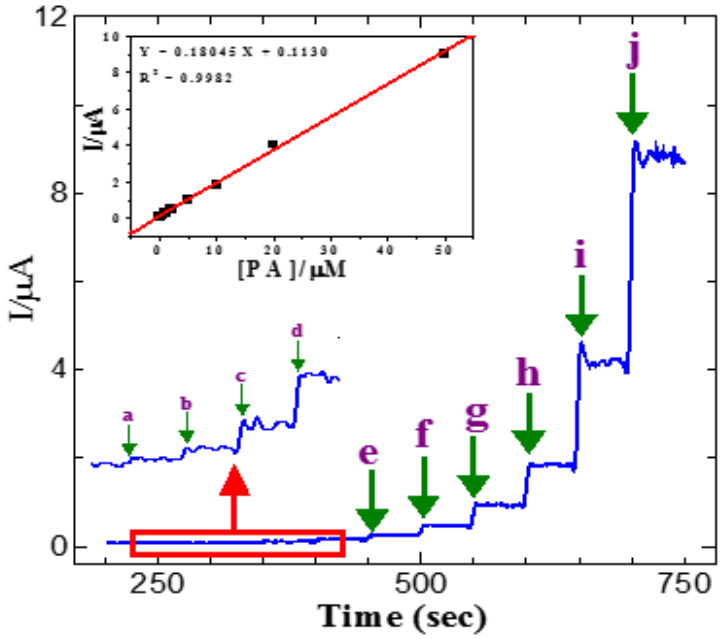

Figure 11. Amperometric i-t curve obtained for (a) 0.03, (b) 0.1, (c) 0.2, (d) 0.5, (e) 1, (f) 2, (g) 5, (h) 10, (i) 10, (j) 20 and (k) 50 μM addition of PA at a constant potential of 0.55 V in 0.2 M PB solution. Inset: Plot of concentration versus the oxidation peak current of PA.

In addition, the present modified electrode is also highly sensitive in the determination of PA in a wide concentration range (0.03 μM – 50 μM) (Figure 11). The plot of PA concentration versus oxidation peak current is linear, with a correlation coefficient of 0.9982. These results indicate that the CuNWs modified electrode is highly sensitive for detecting PA at low concentrations, as well as across a wide concentration range. The high sensitivity of PA determination is possible due to the high electrochemical active surface area provided by CuNWs besides its high electrical conductivity.

CONCLUSION

In this present investigation, CuNWs were successfully synthesized via template assisted synthesis using the HDA as surfactant and stabilizing agent and glucose as a reducing agent. It was found that the growth of CuNWs were not observed either in the absence of glucose or HDA. The surfactant concentration for the growth of CuNWs was optimized to 180 mM. The as-synthesized CuNWs were characterized using UV-vis and FT-IR spectroscopy. FT-IR analysis confirmed the presence of both HDA and glucose on the surface of the CuNWs. The morphological studies were conducted using SEM. It was found that ultra-long CuNWs growth was observed while using 180 mM HDA in the synthesis. The synthesized CuNWs were drop casted on GCE for electrocatalytic applications. The active electrochemical surface area was calculated using Anson equation and it was found to be 0.031 cm^2. The electrocatalytic performance of the GCE/CuNWs was evaluated by investigating the oxidation of paracetamol (PA) under physiological pH conditions. The results revealed a significant enhancement in the oxidation peak current approximately a 5-fold increase when compared to the bare GCE, highlighting the superior catalytic efficiency of the CuNWs. Furthermore, the modified electrode exhibited excellent electrochemical stability, as evidenced by the consistent and reproducible oxidation response of PA over six consecutive potential cycles, indicating its potential for reliable and long-term analytical applications. This could be attributed to the high surface-to-volume ratio of PA, which helps prevent surface fouling caused by its oxidation products. Additionally, the selective determination of PA in the presence of a 100-fold higher concentration of AA was also demonstrated. The present modified electrode is also sensitive towards the determination of 30 nM concentration of PA in addition to the determination of PA in a wide concentration range (30 nM – 50 μM). The high sensitivity and selectivity of PA determination at CuNWs modified electrode could be used to construct PA sensors in the near future.

ACKNOWLEDGEMENT

The authors would like to express their sincere gratitude to Arul Anandar College (Autonomous), Karumathur, Madurai, India for providing the research facilities (DST-FIST lab), seed money research grant (AAC/Dean-Res./Seed Money/097/2024) and continuous support required to carry out this research work successfully.

REFERENCES

1. Rao, R., Pint, C. L., Islam, A. E., Weatherup, R. S., Hofmann, S., Meshot, E. R., Wu, F., Zhou, C., Dee, N., Amama, P. B., Carpena-Nuñez, J., Shi, W., Plata, D. L., Penev, E. S., Yakobson, B. I., Balbuena, P. B., Bichara, C., Futaba, D. N., Noda, S., Shin, H., Kim, K. S., Simard, B., Mirri, F., Pasquali, M., Fornasiero, F., Kauppinen, E. I., Arnold, M., Cola, B. A., Nikolaev, P., Arepalli, S., Cheng, H. -M., Zakharov, D. N., Stach, E. A., Zhang, J., Wei, F., Terrones, M., Geohegan, D. B., Maruyama, B., Maruyama, S., Li, Y., Adams, W. W. and Hart, A. J. (2018) Carbon nanotubes and related nanomaterials: critical advances and challenges for synthesis toward mainstream commercial applications. *ACS Nano*, **12**, 11756–11784.

2. Saber, N. B., Mezni, A., Alrooqi, A. and Altalhi, T. (2020) A review of ternary nanostructures based noble metal/semiconductor for environmental and renewable energy applications. *Journal of Materials Research and Technology*, **9**, 15233–15262.

3. Garnett, E., Mai, L. and Yang, P. (2019) Introduction: 1D Nanomaterials/Nanowires. Chemical Reviews, **119**, 8955−8957.

4. Jin, T., Han, Q., Wang, Y. and Jiao, L. (2018) 1D Nanomaterials: Design, synthesis, and applications in sodium–ion batteries. *Small*, **14**, 1703086.

5. Li, Y., Yang, X. -Y., Feng, Y., Yuan, Z. -Y. and Su, B. -L. (2012) One-Dimensional Metal Oxide Nanotubes, Nanowires, Nanoribbons, and Nanorods: Synthesis, Characterizations, Properties and Applications. *Critical Reviews in Solid State and Materials Sciences*, **37**, 1–74.

6. Machín, A., Fontánez, K., Arango, J. C., Ortiz, D., De León, J., Pinilla, S., Nicolosi, V., Petrescu, F. I., Morant, C. and Márquez, F. (2021) One-Dimensional (1D) Nanostructured Materials for Energy Applications. *Materials*, **14**, 2609.

7. Weng, B., Liu, S., Tang, Z. -R. and Xu, Y. -J. (2014) One-dimensional nanostructure based materials for versatile photocatalytic applications. *RSC Advances*, **4**, 12685–12700.

8. Zhai, T. and Yao, J. (2013) One-dimensional nanostructures: Principles and applications. *John Wiley & Sons, Inc., Hoboken, New Jersey*.

9. Sarkar, J., Khan, G. G. and Basumallick, A. (2007) Nanowires: properties, applications and synthesis via porous anodic aluminium oxide template. *Bulletin of Materials Science*, **30**, 271–290.

10. Ambhorkar, P., Wang, Z., Ko, H., Lee, S., Koo, K. -I., Kim, K. and Cho, D. D. (2018) Nanowire-based biosensors: From growth to applications. *Micromachines (Basel)*, **12**, 679.

11. Barrigón, E., Heurlin, M., Bi, Z., Monemar, B. and Samuelson L. (2019) Synthesis and Applications of III–V Nanowires. *Chemical Reviews*, **119**, 9170–9220.

12. Khan, I., Saeed, K. and Khan, I. (2019) Nanoparticles: Properties, applications and toxicities. *Arabian Journal of Chemistry*, **12**, 908–931.

13. Bhagat, M., Anand, R., Sharma, P., Rajput, P., Sharma, N. and Singh, K. (2021) Review - Multifunctional Copper Nanoparticles: Synthesis and Applications. *ECS Journal of Solid State Science and Technology*, **10**, 063011.

14. Manikandan, A., Lee, L., Wang, Y. -C., Chen, C. -W., Chen, Y. -Z., Medina H., Tseng J. -Y., Wang, Z. M. and Chueh, Y. -L. (2017) Graphene-coated copper nanowire networks as a highly stable transparent electrode in harsh environments toward efficient electrocatalytic hydrogen evolution reactions. *Journal of Materials Chemistry A*, **5**, 13320–13328.

15. Bhanushali, S., Jason, N. N., Ghosh, P. C., Ganesh, A., Simon, G. P. and Cheng, W. (2017) Enhanced Thermal Conductivity of Copper Nanofluids: The Effect of Filler Geometry. *ACS Applied Materials & Interfaces*, **9**, 18925–18935.

16. Li, X., Wang, Y., Yin, C. and Yin, Z. (2020) Copper nanowires in recent electronic applications: progress and perspectives. *Journal of Materials Chemistry C*, **8**, 849–872.

17. Nam, V. B. and Lee, D. (2016) Copper Nanowires and Their Applications for Flexible, Transparent Conducting Films: A Review. *Nanomaterials (Basel)*, **6**, 47.

18. Mott, D., Galkowski, J., Wang, L., Luo, J. and Zhong, C. -J. (2007) Synthesis of Size-Controlled and Shaped Copper Nanoparticles. *Langmuir*, **23**, 5740–5745.

19. Aissa, M. A. B., Tremblay, B., Andrieux-Ledier, A., Maisonhaute, E., Raouafi, N. and Courty, A. (2015) Copper nanoparticles of well-controlled size and shape: a new advance in synthesis and self-organization. *Nanoscale*, **7**, 3189–3195.

20. Jeong, S., Liu, Y., Zhong, Y., Zhan, X., Li, Y., Wang, Y., Cha, P. M., Chen, J. and Ye, X. (2020) Heterometallic Seed-Mediated Growth of Monodisperse Colloidal Copper Nanorods with Widely Tunable Plasmonic Resonances. *Nano Letters*, **20**, 7263–7271.

21. Wang, Y., Shen, H., Livi, K. J. T., Raciti, D., Zong, H., Gregg, J., Onadeko, M., Wan, Y., Watson, A. and Wang, C. (2019) Copper Nanocubes for CO_2 Reduction in Gas Diffusion Electrodes. *Nano Letters*, **19**, 8461–8468.

22. Luc, W., Fu, X., Shi, J., Lv, J. -J., Jouny, M., Ko, B. H., Xu, Y., Tu, Q., Hu, X., Wu, J., Yue, Q., Liu, Y., Jiao, F. and Kang, Y. (2019) Two-dimensional copper nanosheets for electrochemical reduction of carbon monoxide to acetate. *Nature Catalysis*, **2**, 423–430.

23. Cui, F., Yu, Y., Dou, L. T., Sun, J. W., Yang, Q., Schildknecht, C., Schierle-Arndt, K. and Yang, P. D. (2015) Synthesis of Ultrathin Copper Nanowires Using Tris(trimethylsilyl)silane for High-Performance and Low-Haze Transparent Conductors. *Nano Letters,* **15**, 7610–7615.

24. Han, S., Hong, S., Ham, J., Yeo, J., Lee, J., Kang, B., Lee, P., Kwon, J., Lee, S. S. and Yang, M. Y. (2014) Fast plasmonic laser nanowelding for a cu-nanowire percolation network for flexible transparent conductors and stretchable electronics. *Advanced Materials*, **26**, 5808–5814.

25. Xu, W. -H., Wang, L., Guo, Z., Chen, X., Liu, J. and Huang, X. -J. (2015) Copper Nanowires as Nanoscale Interconnects: Their Stability, Electrical Transport, and Mechanical Properties. *ACS Nano*, **9**, 241–250.

26. Peng, W. -T., Chen, F. -R. and Lu, M. -C. (2021) Thermal conductivity and electrical resistivity of single copper nanowires. *Physical Chemistry Chemical Physics*, **23**, 20359–20364.

27. Zhang, Y., Guo, J., Xu, D., Sun, Y. and Yan, F. (2018) Synthesis of Ultralong Copper Nanowires for High-Performance Flexible Transparent Conductive Electrodes: The Effects of Polyhydric Alcohols. *Langmuir*, **34**, 3884–3893.

28. Stortini, A. M., Moretto, L. M., Mardegan, A., Ongaro, M. and Ugo, P. (2015) Arrays of copper nanowire electrodes: Preparation, characterization and application as nitrate sensor. *Sensors and Actuators B: Chemical*, **207**, 186–192.

29. Maurer, F., Dangwal, A., Lysenkov, D., Müller, G., Eugenia, M., Molares, T., Trautmann, C., Brötz, J. and Fuess, H. (2006) Field emission of

copper nanowires grown in polymer ion-track membranes. *Nuclear Instruments and Methods in Physics Research B*, **245**, 337–341.

30. Chen, H. -C. and Tuan, H. -Y. (2017) High-performance lithium-ion batteries with 1.5 μm thin copper nanowire foil as a current collector. *Journal of Power Sources*, **346**, 40–48.

31. Gupta, J., Arya, S., Verma, S., Singh, A., Sharma, A., Singh, B. and Sharma, R. (2019) Performance of template-assisted electrodeposited Copper/ Cobalt bilayered nanowires as an efficient glucose and Uric acid sensor. *Materials Chemistry and Physics*, **238**, 121969.

32. Zhao, Y., Zhang, Y., Li, Y. and Yan, Z. (2012) A flexible chemical vapor deposition method to synthesize copper@carbon core–shell structured nanowires and the study of their structural electrical properties. *New Journal of Chemistry*, **36**, 1161–1169.

33. Zhao, S., Han, F., Li, J., Meng, X., Huang, W., Cao, D., Zhang, G., Sun, R. and Wong, C. -P. (2018) Advancements in copper nanowires: synthesis, purification, assemblies, surface modification, and applications. *Small*, **14**, 1800047.

34. Khan, A., Rashid, A., Younas, R. and Chong, R. (2016) A chemical reduction approach to the synthesis of copper nanoparticles. *International Nano Letters*, **6**, 21–26.

35. Kevin, M., Limb, G. Y. R. and Ho, G. W. (2015) Facile control of copper nanowire dimensions via the Maillard reaction: using food chemistry for fabricating large-scale transparent flexible conductors. *Green Chemistry*, **17**, 1120–1126.

36. Guo, H., Lin, N., Chen, Y., Wang, Z., Xie, Q., Zheng, T., Gao, N., Li, S., Kang, J., Cai, D. and Peng, D. -L. (2013) Copper Nanowires as Fully Transparent Conductive Electrodes. *Scientific Reports*, **3**, 2323.

37. Liu, Z., Yang, Y., Liang, J., Hu, Z., Li, S., Peng, S. and Qian, Y. (2003) Synthesis of Copper Nanowires via a Complex-Surfactant-Assisted Hydrothermal Reduction Process. *Journal of Physical Chemistry B*, **107**, 12658–12661.

38. Kumar, D. V. R., Woo, K. J. and Moon, J. (2015) Promising wet chemical strategies to synthesize Cu nanowires for emerging electronic applications. *Nanoscale*, **7**, 17195–17210.

39. Giannousi, K., Lafazanis, K., Arvanitidis, J., Pantazaki, A. and Dendrinou-Samara, C. (2014) Hydrothermal synthesis of copper based nanoparticles: antimicrobial screening and interaction with DNA. *Journal of Inorganic Biochemistry*, **133**, 24–32.

40. Wang, Y., Liu, P., Zeng, B., Liu, L. and Yang (2018) Facile Synthesis of ultralong and thin copper nanowires and its application to high-performance flexible transparent conductive electrodes. *Nanoscale Research Letters*, **13**, 78.

41. Hwang, C., Baeg, J., An, J., Kim, M. -G., Choi, B. D., Ok, K. M., Kim, K. and Hong, J. (2016) Controlled aqueous synthesis of ultra-long copper nanowires for stretchable transparent conducting electrode. *Journal of Materials Chemistry C*, **4**, 1441–1447.

42. Mayousse, C., Celle, C., Carella, A. and Simonato, J. -P. (2014) Synthesis and purification of long copper nanowires. Application to high performance flexible transparent electrodes with and without PEDOT:PSS. *Nano Research*, **7**, 315–324.

43. Zheng, Y., Chen, N., Wang, C., Zhang, X. and Liu, Z. (2018) Oleylamine-Mediated Hydrothermal Growth of Millimeter-Long Cu Nanowires and Their Electrocatalytic Activity for Reduction of Nitrate, *Nanomaterials*, **8**,192.

44. Aziz, A., Zhang, T., Lin, Y. -H., Daneshvar, F., Sue, H. -J. and Welland, M. E. (2017) 1D copper nanowires for flexible printable electronics and high ampacity wires. *Nanoscale*, **9**, 13104–13111.

45. McCrae, J. C., Morrison, E. E., MacIntyre, I. M., Dear, J. W. and Webb, D. J. (2018) Long-term adverse effects of paracetamol - a review. *British Journal of Clinical Pharmacology*, **84**, 2218–2230.

46. Prescott, L. F. (1980) Kinetics and metabolism of paracetamol and phenacetin. *British Journal of Clinical Pharmacology*, 10, 291S–298S.

47. Mazaleuskaya, L. L., Sangkuhl, K., Thorn, C. F., Gerald, G. A. F., Altman, R. B. and Klein, T. E. (2015) PharmGKB summary: pathways of acetaminophen metabolism at the therapeutic versus toxic doses. *Pharmacogenetics and Genomics*, **8**, 416–426.

48. Chang, Y., Lye, M. L. and Zeng, H. C. (2005) Large-Scale Synthesis of High-Quality Ultralong Copper Nanowires. *Langmuir*, **21**, 3746–3748.

49. Jena, B. K. and Raj, C. R. (2006) Enzyme-Free Amperometric Sensing of Glucose by Using Gold Nanoparticles. *Chemistry A European Journal*, **12**, 2702–2708.

50. Anson, F. C. (1966) Innovations in the Study of Adsorbed Reactants by Chronocoulometry. *Analytical Chemistry*, **38**, 54–57.

51. Legrand, J., Dumont, E., Comiti, J. and Fayolle, F. (2000) Diffusion coefficients of ferricyanide ions in polymeric solutions — comparison of different experimental methods. *Electrochimica Acta*, **45**, 1791–1803.

52. Bhanushali, S., Ghosh, P., Ganesh, A. and Cheng, W. (2015) 1D Copper Nanostructures: Progress, Challenges and Opportunities. *Small*, **18**, 1232–1252.

53. Gowthaman, N. S. K., Raj, M. A. and John, S. A. (2017) Nitrogen-doped graphene as a robust scaffold for the homogeneous deposition of copper nanostructures: A nonenzymatic disposable glucose sensor. *ACS Sustainable Chemistry & Engineering*, **5**, 1648–1658.

54. Mohl, M., Pusztai, P., Kukovecz, A., Konya, Z., Kukkola, J., Kordas, K., Vajtai, R. and Ajayan, P. M. (2010) Low-temperature large-scale synthesis and electrical testing of ultralong copper nanowires, *Langmuir*, **26**, 16496–502.

55. Shi, Y., Li, H., Chen, L. and Huang, X. (2005) Obtaining ultra-long copper nanowires via a hydrothermal process. *Science and Technology of Advanced Materials*, **6**, 761–765.

56. Na, W., Lee, J., Jun, J., Kim, W., Kim, Y. K., Jang, J. (2019) Highly sensitive copper nanowire conductive electrode for nonenzymatic glucose detection. *Journal of Industrial and Engineering Chemistry*, **69**, 358–363.

57. Jin, M., He, G., Zhang, H., Zeng, J., Xie, Z., Xia, Y. (2011) Shape-Controlled Synthesis of Copper Nanocrystals in an Aqueous Solution with Glucose as a Reducing Agent and Hexadecylamine as a Capping Agent. *Angewandte Chemie*, **50**, 10560–10564.

58. Liu, X., Yang, C., Yang, W., Lin, J., Liang, C., Zhao, X. (2021) One-pot synthesis of uniform Cu nanowires and their enhanced non-enzymatic glucose sensor performance. *Journal of Materials Science*, **56**, 5520–5531.

59. Zhang, D., Wang, R., Wen, M., Weng, D., Cui, X., Sun, J., Li, H. and Lu, Y. (2012) Synthesis of ultralong copper nanowires for high-performance transparent electrodes. *Journal of the American Chemical Society*, **134**, 14283–14286.

60. Chen, S. and Sommers, J. M. (2001) Alkanethiolate-Protected Copper Nanoparticles: Spectroscopy, Electrochemistry, and Solid-State Morphological Evolution. *Journal of Physical Chemistry B*, **105**, 8816–8820.

61. Male, K. B., Hrapovic, S., Liu, Y., Wang, D. and Luong, J. H. T. (2004) Electrochemical detection of carbohydrates using copper nanoparticles and carbon nanotubes. *Analytica Chimica Acta*, **516**, 35–41.